Effect of early Pliocene uplift on late Pliocene cooling in the Arctic–Atlantic gateway

Jochen Knies [a,b,*], Rune Mattingsdal [c,1], Karl Fabian [a,b], Kari Grøsfjeld [a], Soma Baranwal [a,b], Katrine Husum [c], Stijn De Schepper [d], Christoph Vogt [e], Nils Andersen [f], Jens Matthiessen [g], Karin Andreassen [b,c], Wilfried Jokat [g], Seung-Il Nam [h], Carmen Gaina [i]

[a] Geological Survey of Norway, NO-7491 Trondheim, Norway
[b] Centre for Arctic Gas Hydrate, Environment and Climate, University of Tromsø, NO-9037 Tromsø, Norway
[c] University of Tromsø, NO-9037 Tromsø, Norway
[d] University of Bergen, NO-5020 Bergen, Norway
[e] Crystallography/ZEKAM, Geosciences, University of Bremen, DE-28359 Bremen, Germany
[f] Leibniz Laboratory for Radiometric Dating and Stable Isotope Research, University of Kiel, DE-24118 Kiel, Germany
[g] Alfred Wegener Institute Helmholtz Centre for Polar and Marine Research, DE-27568 Bremerhaven, Germany
[h] Korea Polar Research Institute, 406-840 Incheon, Republic of Korea
[i] Centre for Earth Evolution and Dynamics, University of Oslo, NO-0316 Oslo, Norway

A R T I C L E   I N F O

A B S T R A C T

Despite the undisputed role of the Arctic Ocean in the modern and Pliocene climate system, the Arctic has only recently attracted public awareness that ongoing, fundamental change in the Arctic cryosphere could be a response to global warming. Clarification of the Arctic's role in global climate during the Pliocene is, however, largely hampered by equivocal stratigraphic constraints. From a well-dated Pliocene sequence from the Yermak Plateau, off NW Spitsbergen, we present sedimentological and geochemical data indicating that 4 million years ago terrigenous sediment supply and sources changed abruptly in response to a regional tectonic uplift event. We argue that this event together with contemporary uplift and tilting along the northwestern European continental margin preconditioned the landmasses for glacial ice build-up during intensification of the Northern Hemisphere Glaciation (INHG). Our data further suggest that the final deepening/widening of the Arctic–Atlantic gateway, the Fram Strait, between 6.5 and 5 Ma gradually caused increased deep-water mass exchange which, in turn, likely contributed to the intensification of the North Atlantic thermohaline circulation. Coupled to the North Atlantic warm pool as a regional moisture source, declining atmospheric CO_2 levels and other feedback mechanisms during the Pliocene, the regional tectonic activities in the high northern latitudes caused decreased summer ablation and thus allowed the initial build-up of glacial ice both in Scandinavia, and the sub-aerially exposed Svalbard/Barents Sea, culminating in the first large-scale coastline-shelf edge glaciations at ~2.75 Ma ago.

© 2013 Elsevier B.V. All rights reserved.

1. Introduction

The influence of the Arctic Ocean on Pliocene global climate reconstructions has remained ambiguous due to a lack of well-dated paleoenvironmental records. Important topics have still not been resolved, amongst them: (1) the Pliocene climate and tectonic history of the Arctic Ocean (e.g. Matthiessen et al., 2009a); (2) the final development of the gateway as the only deep-water connection to the Arctic Ocean via the Fram Strait (Jakobsson et al., 2007); and (3) the influence of the gateway region on changes in Arctic–Atlantic ocean circulation (Sarnthein et al., 2009), uplift/erosion on the adjacent hinterland (Green and Duddy, 2010; Laberg et al., 2012), as well as glacial initiation and its consequences for the petroleum systems in the region (Henriksen et al., 2011).

This lack of knowledge is mainly due to the ambiguous Plio-Pleistocene stratigraphic framework of the Arctic Ocean (Matthiessen et al., 2009a). Although a late Neogene stratigraphy for the central Arctic Ocean has been constructed from the first scientific drill holes (Integrated Ocean Drilling Program (IODP) Expedition 302 ACEX, e.g. Moran et al., 2006; Backman et al., 2008; Frank et al., 2008; Backman and Moran, 2009), insufficient recovery and limited absolute age control do not allow the establishment of a master stratigraphy for the Plio-Pleistocene (Matthiessen et al.,

* Corresponding author.
[1] Present address: Norwegian Petroleum Directorate, Verkstedveien 1, PO Box 787, NO-9488 Harstad, Norway.
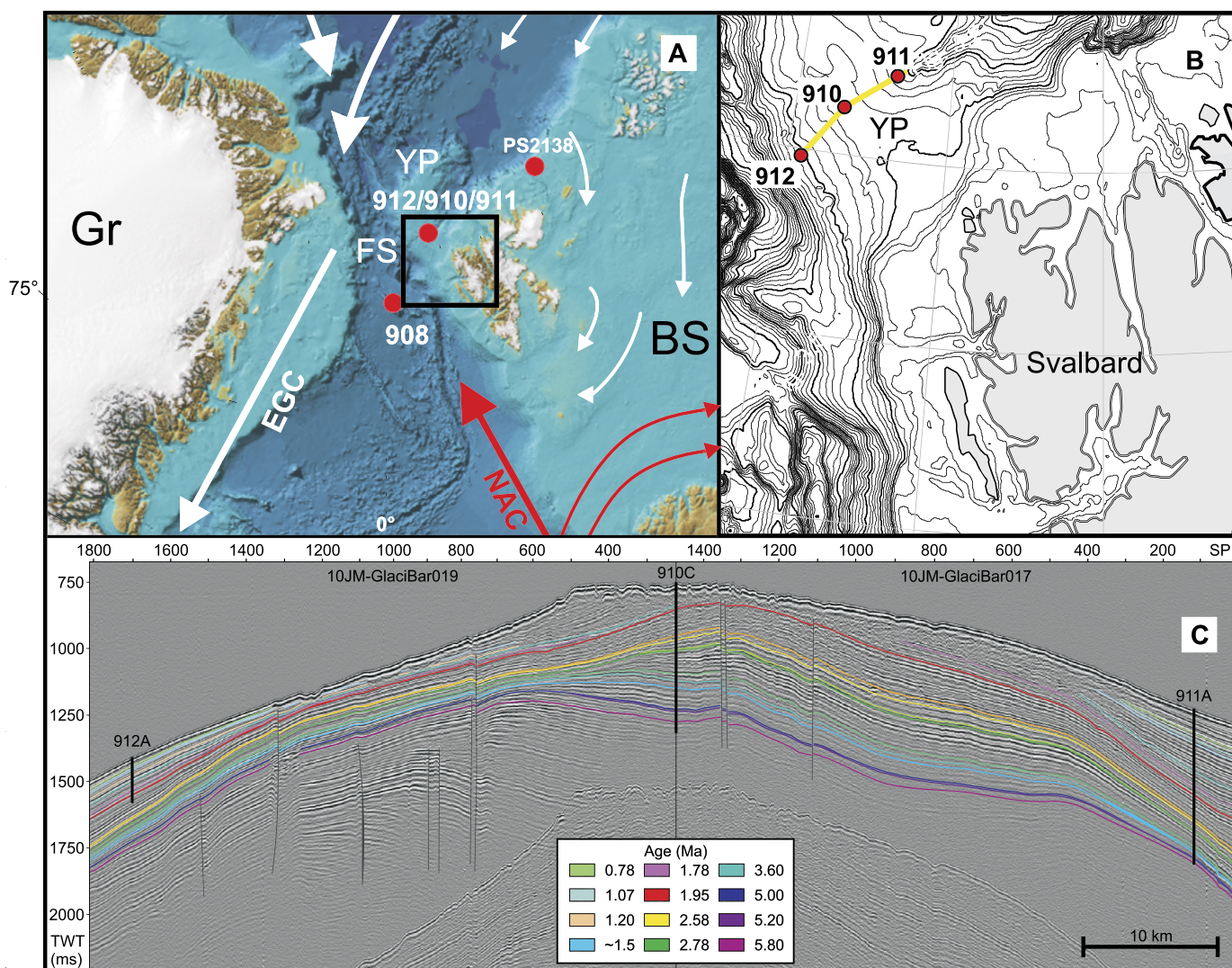
Fig. 1. (A) Physiogeography in the Atlantic–Arctic gateway region and location of investigated Ocean Drilling Program (ODP) sites and reference core PS2138. Red arrows: North Atlantic Current (NAC); white arrows: Transpolar Drift and East Greenland Current (EGC). YP: Yermak Plateau; BS: Barents Sea; FS: Fram Strait. (B) Inset map showing (from west) the location of ODP sites 912, 910, and 911 and the 2D high-resolution single-channel seismic lines 10JM-GlaciBar19 and 10JM-GlaciBar17. (C) Composite seismic profile crossing ODP Holes 912A, 910C and 911A on the Yermak Plateau. Seismic amplitudes with color coded reflectors dated by age fix-points from the three ODP Holes as discussed by Mattingsdal et al. (2013) and detailed in Supplementary Table S1.

2009b; O'Regan et al., 2010; März et al., 2010). More promising are the ODP sites from the marginal Arctic Ocean, i.e. the Atlantic–Arctic gateway region (ODP Leg 151) (Myhre et al., 1995) (Fig. 1). Here, in contrast to the central Arctic Ocean, carbonate bearing sequences permit establishment of a relatively continuous stable oxygen isotope ($\delta^{18}O$) and foraminiferal stratigraphy, which still are the prerequisite for any subsequent application of chronological approaches (Knies et al., 2007). Moreover, the region is characterized by dynamic coupling between the northernmost branch of the North Atlantic Current and the Arctic Ocean allowing inferences on changes of external forcing factors (tectonic activity, freshwater supply) that may have influenced water mass characteristics, circulation and sea ice cover (e.g. Sarnthein et al., 2009; Lunt et al., 2012).

A new stratigraphic framework for the Arctic gateway region over the last 6 Ma has recently been established, using available material from ODP Leg 151 (Sites 910, 911 and 912) and new high-resolution seismic data (Mattingsdal et al., 2013) (Fig. 1). According to this new stratigraphic model, sites 910 and 911 have recovered complete marine Pliocene sequences allowing new inferences and in-situ testing of the proposed early-mid Pliocene Arctic

warming (e.g. Robinson et al., 2011; Ballantyne et al., 2010), the final opening of the Atlantic–Arctic gateway (e.g. Kristoffersen, 1990; Engen et al., 2008), and the onset and intensification of the Northern Hemisphere Glaciation (INHG) between ∼3.6 and 2.7 Ma (Mudelsee and Raymo, 2005).

In this paper, we focus on the Pliocene epoch (∼5.332–2.588 Ma) (Gradstein et al., 2012) and discuss onset and intensification of the Northern Hemisphere glaciations, as well as regional tectonic constraints in the gateway region during its final opening, from a consistent Pliocene stratigraphic framework of Hole 910C and 911A (Fig. 1). New stable isotope and multi-proxy data are discussed with previously published results from the Fram Strait (ODP Site 908) (Matthiessen et al., 2009a; Winkler et al., 2002; Wolf-Welling et al., 1996), the southwestern Barents Sea (Ryseth et al., 2003), and the NW European margin (Stoker et al., 2002, 2005; Dahlgren et al., 2005; Eidvin et al., 2007). We provide stratigraphic evidence that passive margin uplifts during the late Miocene/early Pliocene preconditioned the landscape adjacent to a warm Pliocene North Atlantic Ocean for continental ice sheet growth around 4 Ma. The new results support the hypothesis put forward in previous studies (Ruddiman and Kutzbach, 1989;

Eyles, 1996; Foster et al., 2010) that late Miocene/early Pliocene uplift in regions sensitive to orbitally forced changes in solar radiation was one decisive trigger for the permanent persistence of glacial ice in the Northern Hemisphere. Together with the decline in atmospheric pCO$_2$ (Lunt et al., 2008; Bartoli et al., 2011; Seki et al., 2010), and changes in meridional overturning circulation (MOC) as response to the closure of the Central American Seaways (CAS) during the Pliocene (Driscoll and Haug, 1998; Sarnthein et al., 2009; De Schepper et al., 2013), non-glacial, tectonic uplift of mountains and plateaus in far-off polar regions during the early Pliocene may indeed be important to explain the intensification of the Northern Hemisphere Glaciation at 2.75 million years ago (Ruddiman, 2010).

2. Material and methods

ODP Hole 910C was drilled in 556.4 m water depth on the southern Yermak Plateau (80°15.896'N, 6°35.430'E). In total, 507.4 m of sediments were cored, and recovery was 57% on average, with 80% between 170 and 504.7 m below seafloor (mbsf) (Myhre et al., 1995). The borehole was re-sampled between 150 and 504.7 mbsf for stable isotope (116 samples), and inorganic geochemical as well as sedimentological analyses (443 samples). ODP Hole 911A was drilled in 901.6 m water depth (80°28.466'N, 8°13.640'E). 505.8 m of sediments were cored with an average core recovery of 91.8% (Myhre et al., 1995). The borehole was re-sampled for paleomagnetic measurement between 340 and 505 mbsf to complete the initial results from the shipboard analyses (Myhre et al., 1995). For the same interval, grain size and major/trace element analyses were conducted (430 samples). In order to compare previously analyzed clay minerals from Hole 911A (Knies et al., 2009), Hole 908A from the Hovgård Ridge, central Fram Strait (78°23.112'N, 1°21.637'E) (Fig. 1) was re-sampled (47 samples) between 90 and 183 mbsf and analyzed for clay minerals applying identical methodological procedures. The predicted paleobathymetry at 6.5 and 2.5 Ma (Gradstein et al., 2012) in the Fram Strait has been constructed using the method from Brown et al. (2006) and Müller et al. (2008). Depth reconstruction to basement is based on a new regional kinematic model and guided by the interpretation of new magnetic data (Ehlers and Jokat, 2009). The new isochrones have been merged with the regional kinematic model published in Knies and Gaina (2008). Detailed information on the analytical techniques and paleobathymetric reconstruction are in the Supplementary Materials.

3. The Pliocene chronology

Supported by new high-resolution seismic data (Fig. 1), Mattingsdal et al. (2013) recently developed a new age model for ODP Holes 910C and 911A. This new model was further confirmed by additional biostratigraphic datums for the base of Hole 911A (Grøsfjeld et al., 2013). Here, we summarize the findings of both studies and supplement the new age model with additional benthic stable isotope data from Hole 910C providing the most up to date and consistent Pliocene stratigraphic framework for the European sector of the marginal Arctic Ocean.

The Plio-Pleistocene boundary in Hole 910C and 911A is constrained by the biostratigraphic "Datum A" at 2.78 Ma at 223 and 391.9 mbsf, respectively (Supplementary Fig. S1, Table S1) (Sato and Kameo, 1996; Sato et al., 2004). It is further supported by the Matuyama–Gauss boundary at 361.33 mbsf in Hole 911A (Supplementary Fig. S1). Below, the lowest occurrence (LO) of the acritarch *Lavradosphaera crista* at 505.64 mbsf in Hole 911A provides a maximum age of ~5.8 Ma (Grøsfjeld et al., 2013). This datum was established at DSDP Hole 603C in the mid-latitudes of the Western North Atlantic (De Schepper and Head, 2013). At higher latitude
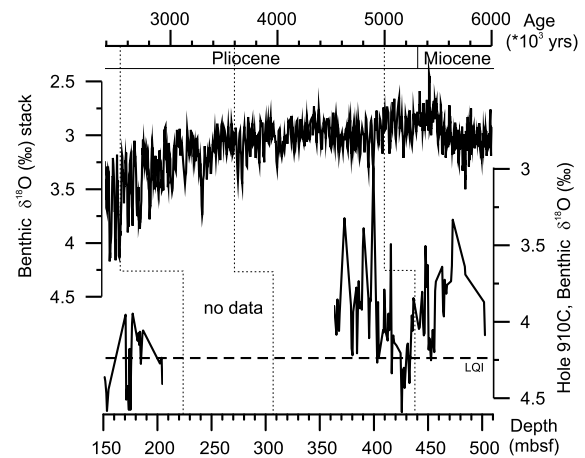

Fig. 2. Late Miocene to Pliocene global benthic oxygen isotope records (Zachos et al., 2001; Lisiecki and Raymo, 2005) compared to stable oxygen isotope data derived from the benthic foraminifera *Cassidulina teretis* in Hole 910C. Note that data are not available between 210 and 360 mbsf. Vertical dotted lines indicate age-depth stratigraphic fix-points as outlined in Table S1. Dashed horizontal line indicates late Quaternary interglacial (LQI) isotopic mean value of benthic foraminifera *Cassidulina teretis* in sediment core PS2138 (Wollenburg et al., 2001, Tine Rasmussen, personal communication, 2012).

sites, the lowest occurrence is recorded at ~4.9 Ma in the Iceland Sea (Schreck et al., 2012), at ~4.8 Ma in the Norwegian Sea (De Schepper and Head, 2013) and at ~5.3 Ma near the Miocene–Pliocene boundary in the Labrador Sea (De Schepper and Head, 2013). The occurrence of *Barssidinium evangelineae* between 477.83 and 505.64 mbsf in ODP 911A indicates an age no younger than 5.0 Ma for the base of the core (Grøsfjeld et al., 2013), as the recorded age range of this species is between 8.8 and ca. 5.0 Ma (Powell and Brinkhuis, 2004). The occurrence of *B. evangelineae* and *L. crista* in the lower part of Hole 911A indicates an age between ~5.8 and 5.0 Ma. The latter agrees well with the highest occurrence (HO) of planktonic foraminifers *Globigerina praebulloides* at 488.1 mbsf and *Paragloborotalia continuosa* (single specimen) at 491.4 mbsf restricting the time frame of the lower part of Hole 911A close to the Miocene/Pliocene transition (Spiegler, 1996; Mattingsdal et al., 2013). The base of Hole 911A is in a normal polarity chron correlated to the Thvera subchron (Supplementary Fig. S1). By linearly extrapolating the sedimentation rate model from the latest tie-point of 5.00 Ma (Top Thvera) at 492.42 mbsf, we achieve a base age of ~5.2 Ma.

The correlation of the 5.00 Ma seismic reflector into Hole 910C at 438 mbsf (see Mattingsdal et al., 2013) indicates that Hole 910C has recovered older sediment sequences (Fig. 1). The LO of the dinocyst *Selenopemphix islandensis* at 408.3 mbsf indicates an age between ~4.5 (Verhoeven and Louwye, 2012) and ~5.5 Ma (ODP 642, S. De Schepper, unpublished data). The acritarch *Lavradosphaera crista* was first recorded at 450 mbsf, providing a maximum age of ~5.8 Ma, or possibly 4.8–5.3 Ma when considering its range at higher latitude ocean sites. Supporting evidence of an age no older than late Miocene comes from the persistent co-occurrence of acritarchs *Lavradosphaera crista* and *Cymatiosphaera? invaginata*, which has a stratigraphic range from the late Miocene to the Pleistocene (Head et al., 1989). The presence of the calcareous nannofossil *Helicosphaera sellii* at the base of Hole 910C sets a maximum age of ⩽6.5 Ma (Iaccarino et al., 2008).

From additional fix-points (Supplementary Table S2) derived from correlating global stacks of δ^{18}O records (Zachos et al., 2001; Lisiecki and Raymo, 2005) with new benthic δ^{18}O data of Hole 910C (Fig. 2) we further propose that the base of Hole 910C is ~5.8 Ma old. Stable oxygen isotope data of the benthic foraminifera *Cassidulina teretis* in Hole 910C are available for
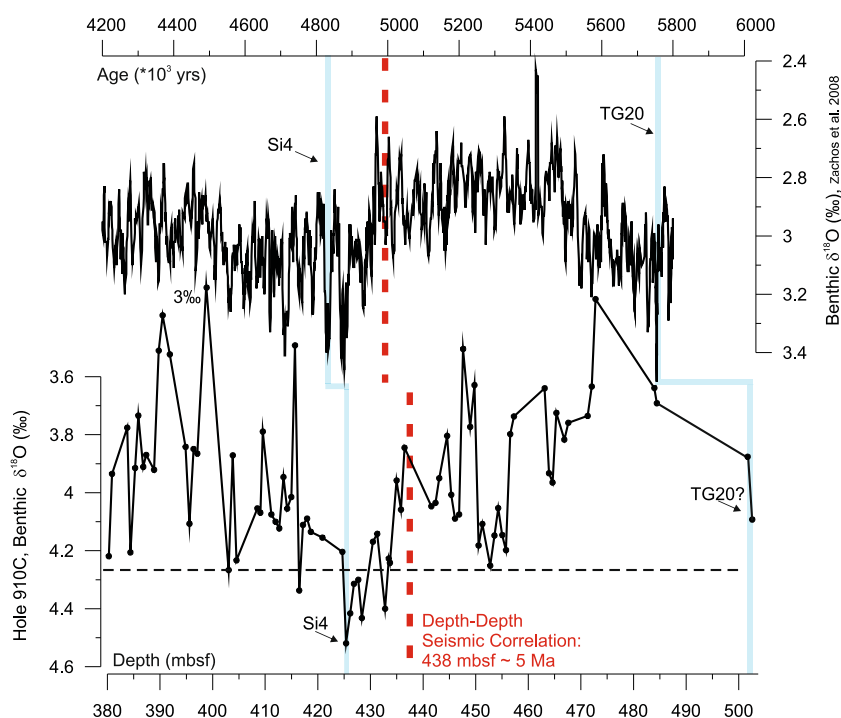
Fig. 3. Correlation of age tie-points between late Miocene/early Pliocene global isotope stack (Zachos et al., 2001) and the benthic isotope record of Hole 910C. Red stippled line marks the tie-point at ∼5 Ma derived from seismic correlation between Top Thvera in Hole 911A and Hole 910C. Blue lines indicate the tie-points for the marine isotope events Si4 and TG20. Black stippled line marks the LQI isotopic mean value for *Cassidulina teretis*. (For interpretation of the references to color in this figure legend, the reader is referred to the web version of this article.)

the Plio-Pleistocene boundary and the late Miocene/early Pliocene transition, and are compared with mean late Quaternary interglacial values from the northeastern Svalbard margin (Wollenburg et al., 2001) (Fig. 2). The results show a gradual trend from lower (∼3.5–4.0‰) to higher δ^{18}O values (∼4.0–4.5‰) from the late Miocene to the late Pliocene, supporting the pattern elsewhere observed in the Nordic seas (e.g. Fronval and Jansen, 1996) with similar or significantly less ice volume occurring during the Miocene/Pliocene compared to the late Pliocene (Zachos et al., 2001) (Fig. 2). By using all age-control points derived from paleomagnetics and biostratigraphy between 2.5 and 5 Ma, a comparison of a δ^{18}O reference curve (LR04) (Lisiecki and Raymo, 2005) with the Yermak Plateau record shows that major global ice volume changes are detectable in the Miocene/Pliocene sequence (Fig. 2). Identification of oxygen isotope events is based on the general agreement that high δ^{18}O > 4‰ associated with relatively high δ^{13}C values characterize glacial isotope stages (Knies et al., 2007). Ages are according to Lisiecki and Raymo (2005). We argue that the tie-point at 438 mbsf (∼5.0 Ma) inferred from seismic correlation between Hole 910C and 911A marks the boundary between two intervals characterized by higher (∼4.9–4.6 Ma) and lower δ^{18}O values (∼5.5–5.0 Ma) (Zachos et al., 2001; Lisiecki and Raymo, 2005) (Fig. 3). The marine isotope stage event Si4 (∼4.85 Ma) has been identified at 425 mbsf (Fig. 3). However, limited data points at the base of Hole 910C make the definition of further tie-points problematic. By linearly extrapolating the sedimentation rate from the latest tie-point (Si4: ∼4.85 Ma) towards the base of Hole 910C, we achieve a base age of ∼5.7 Ma. Hence, we suggest that the high δ^{18}O value at 502.6 m corresponds to the marine isotope stage event TG20 at ∼5.75 Ma (Hodell et al., 2001) (Fig. 3). The base of Hole 910C is tentatively dated to be ∼5.81 Ma.

The Plio-Pleistocene boundary in Hole 910C is constrained by tie-points at ∼190 mbsf (2.58 Ma; Matuyama/Gauss (M/G) boundary) inferred from seismic correlation between Hole 910C and 911A (Mattingsdal et al., 2013), and the biostratigraphic "Datum A" (2.78 Ma) at ∼223 mbsf (Sato and Kameo, 1996) (Fig. 4). Addi-
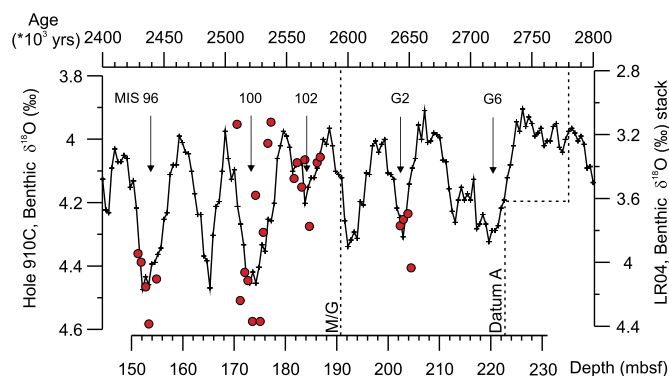

Fig. 4. Compilation of LR04 global isotope stack (age scale) and benthic isotope record (red dots) of Hole 910C (depth scale) during the late Pliocene (2.8–2.4 Ma). The age-depth correlation of the Matuyama/Gauss (M/G) chron boundary and nannofossil "Datum A" sensu Sato and Kameo (1996) are indicated. (For interpretation of the references to color in this figure legend, the reader is referred to the web version of this article.)

tional tie-points can be inferred from glacial-to-interglacial δ^{18}O oscillations of the new benthic δ^{18}O record (Fig. 4). The stable isotope record exhibits distinct cycles between heavy and light values with a gradual increase to heavier values above the M/G boundary. By assuming constant sedimentation rates across the M/G boundary, we identify marine isotope stage (MIS) 96, 100, 102 above the M/G boundary, and MIS G2 below (Fig. 4). All stages resemble the structures displayed in LR04 although with lower amplitudes between glacial and interglacial (max. 0.6‰; MIS 101/100 boundary) (Fig. 4). All age fix-points for Hole 910C and 911A are summarized in the Supplementary Material (Tables S1 and S2).

4. Proxy data

The amount of ice-rafted debris (IRD) in Arctic sediments is commonly used as one decisive proxy to infer the glaciation
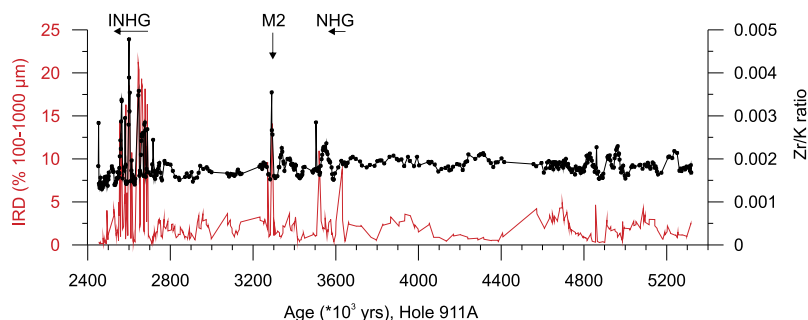
Fig. 5. IRD (wt.%) and Zr/K ratio in bulk sediments of Hole 911A. The onset of the Northern Hemisphere Glaciation (NHG) at ∼3.6 Ma sensu Mudelsee and Raymo (2005), the MIS M2 glaciation at ∼3.3 Ma, and the intensification of NHG (INHG) at ∼2.7 Ma are highlighted.

history of the circum-Arctic during the Plio-Pleistocene. Different approaches and various IRD fractions (wt.% > 63 µm, >125 µm, >500 µm, No. grains/10 ccm > 2 mm) have been applied (Hebbeln et al., 1998; Stein, 2008). In this study, we used the 100–1000 µm size fraction (in wt.%) to represent the IRD signal. For Hole 910C we used the larger grain size fraction 500–1000 µm to measure the IRD supply, since fine to medium sands in this shallower site (556.4 m water depth) may be the result of other sedimentary transport processes (see discussion below). In order to constrain the provenance of the coarse-grained material, we consider sedimentary zirconium (Zr) and titanium (Ti) contents normalized over potassium (K), as often outlined in grain sized specific investigations of terrigenous sediments (e.g. Nizou et al., 2011). Sediment provenance is further constrained by two specific source rock indicators in the clay fraction (<2 µm), i.e. the smectite/illite ratio and relative amounts of gibbsite (Holmes, 1998; Wahsner et al., 1999). Shipboard carbon/nitrogen (C/N) ratios in sediments of Hole 910C (Myhre et al., 1995) supported by published organic carbon stable carbon isotopes ($\delta^{13}C_{Org}$) of Pliocene sediments in Hole 911A (Knies et al., 2002) are used as an organic matter source indicator (Stein and Macdonald, 2004). Detailed information on the usage and limitation of the applied proxies are in the Supplementary Materials and further illustrated in Supplementary Figs. S2–S6.

5. Results and discussion

5.1. Evidence for the INHG in the European Arctic

Both Arctic and sub-Arctic terrestrial and marine records provide consistent evidence for the INHG since the Mid-Pliocene (see Matthiessen et al., 2009a, for review). According to Mudelsee and Raymo (2005) the transition was likely gradual between 3.6 and 2.4 Ma, rather than abrupt. By revising the IRD records in the North Atlantic and the Nordic Seas, Kleiven et al. (2002) show temporal and spatial differences in initial supply from the circum-North Atlantic ice sheets since 3.6 Ma, but fluctuations of all major ice sheets were synchronous since 2.75–2.72 Ma. Into the Arctic Ocean, the IRD record of Hole 911A provides a regional view on the extent of the northern Svalbard/Barents Sea Ice Sheet (SBIS) beyond the coastline and probably towards the shelf edge, but more importantly offers insight into a full sequence of long-term and major trends in the evolution of NHG for the Arctic. We have registered three major IRD events between ∼5.3 and ∼2.5 Ma: (1) during onset of NHG (∼3.6 Ma) sensu Mudelsee and Raymo (2005), (2) during marine isotope stage (MIS) M2, the first major global glacial event sometimes referred to as a "failed attempt at NH glaciation" at ca. 3.3 Ma (Haug and Tiedemann, 1998, De Schepper et al., 2009, 2013) and (3) during glacial MIS G6/4 around 2.7 Ma (Lisiecki and Raymo, 2005) (Fig. 5). All events are regarded as severe glaciations with oxygen isotope values characteristic of

early Quaternary glaciations (Lisiecki and Raymo, 2005). The IRD maxima correspond to enhanced Zr/K ratios, illustrating enhanced supply of glacially derived coarse-grained material from northern Svalbard; the nearest point source for zirconium (Supplementary Fig. S5) (Ottesen et al., 2010). Moderate to low IRD supply during the remaining parts of the Pliocene sequence excludes the presence of glacial ice close to the coastline (Fig. 5). The latter corroborates inferences of predominantly isolated to small-scale mountainous glaciations between ∼7 and ∼3 Ma in the circum-Arctic and Nordic Seas (e.g. Geirsdóttir, 2004; Fronval and Jansen, 1996; Matthiessen et al., 2009a). It further supports evidence of mostly sandy sediments deposited along the NW European continental margin prior to 2.7 Ma as a result of predominantly nonglacial (NW Britain) (Dahlgren et al., 2005; Stoker et al., 2005) or glaciofluvial environments (Svalbard) that controlled the sediment transport to the shelf break (Svalbard) (Forsberg et al., 1999; Butt et al., 2000; Laberg et al., 2010). The abrupt cooling and severe glaciation during MIS M2 (∼3.3 Ma) interrupted this less glaciated period during the Pliocene. It has recently been linked to a weakened North Atlantic Current and reduced heat transport in response to enhanced Pacific to Atlantic through-flow via the CAS (De Schepper et al., 2013). The timing agrees with the inferred ice expansion of the West Antarctic Ice Sheet following a period (∼4.5–3.3 Ma) of smaller ice sheets and reduced sea ice coverage (Naish et al., 2009; McKay et al., 2012). It suggests a synchronous behavior of the ice sheets in the Northern Hemisphere and West Antarctica. Deduced from the IRD records in the Atlantic–Arctic gateway, we propose that ice sheets in the circum-Arctic advanced at least twice beyond the coastline (or even shelf edge), i.e. during MIS M2 and the INHG around 2.75 Ma.

Detailed inspection of the INHG records from the Yermak Plateau places the first shelf edge type glaciations of the ice sheets in the northern Barents Sea within MIS G6 (∼2.74 Ma) (Fig. 6) (Lisiecki and Raymo, 2005); a timing consistent with the final closure of the CAS (Kameo and Sato, 2000; Schmidt, 2007; Sarnthein et al., 2009) and the onset of major NHG as first described by Shackleton et al. (1984). Distinct IRD pulses with a northern Svalbard signature of high Zr/K ratios are recorded during termination of MIS G6, suggesting that this deglaciation pattern showed already a similar pattern as that known from the late Quaternary in the region (Elverhøi et al., 1995; Kleiber et al., 2000; Winkelmann et al., 2008). Subsequent IRD pulses recorded in Hole 911A provide further evidence for repetitive shelf edge glaciations between MIS G4 and MIS 100 (Fig. 6). IRD pulses occur both during glacial advances (high $\delta^{18}O$) and retreats (low $\delta^{18}O$) (Fig. 6). Prior to MIS G6, IRD is absent except for the precursor events at ∼3.3 Ma (M2 glaciation) and around 3.6 Ma, the onset of global cooling sensu Mudelsee and Raymo (2005) (Fig. 5). Accordingly, melting icebergs sourced from the Svalbard/Barents Sea Ice Sheet are not a major component in the North Atlantic IRD record prior to 2.74 Ma (Laberg et al., 2010). An abrupt culmination
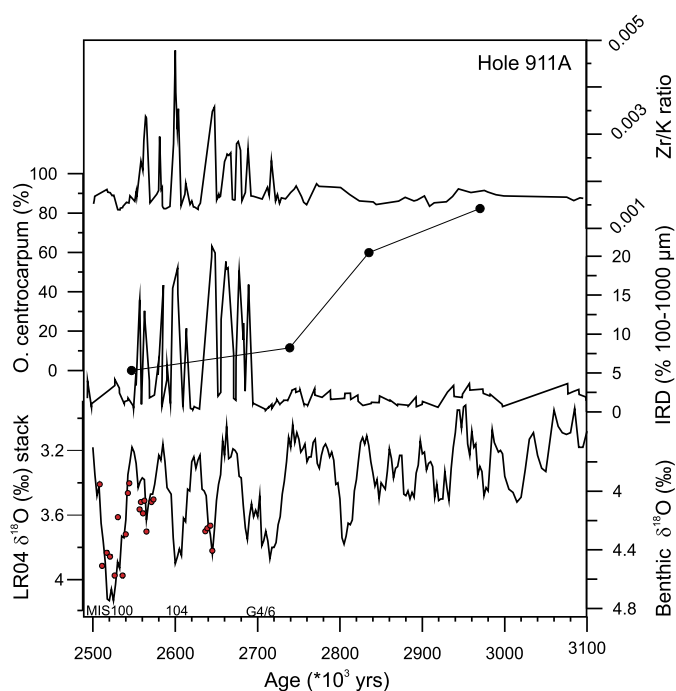
Fig. 6. The INHG in the Atlantic–Arctic gateway region exemplified by proxy data of Hole 911A. From top to bottom: Zr/K ratio and IRD (wt.% 100–1000 μm) records as well as percentages of dinoflagellate cyst *Operculodinum centrocarpum* between 2.5 and 3.1 Ma. Benthic $\delta^{18}O$ record (Hole 910C) superimposed on LR04 global isotope stack (Lisiecki and Raymo, 2005) (MIS100, 104, and G4/G6 are displayed).

in glacial ice build-up beyond the coastline at 2.74 Ma is also recorded and precisely dated in both the sub-Arctic Northwest Pacific (Haug et al., 2005), and the northern North Atlantic (Bartoli et al., 2005). Bartoli et al. (2005) argued that the surface water warming between 2.95 and 2.82 Ma in the northern North Atlantic is associated with a stronger thermohaline circulation and northward heat transport, providing an additional moisture supply that ultimately led to the INHG at 2.74 Ma (MIS G6). Significant occurrences of the dinoflagellate cyst *Operculodinum centrocarpum* in sediments deposited prior to 2.74 Ma reflect the presence of North Atlantic Current derived warm water masses on the Yermak Plateau (Fig. 6) (Knies et al., 2002). This illustrates how the inflow of warm water masses associated with the closure of the CAS had a significant impact on the build-up of continental ice sheets in the Atlantic–Arctic gateway region (Sarnthein et al., 2009). Other mechanisms that likely contributed to the major INHG at 2.74 include declining pCO$_2$ concentrations (Lunt et al., 2008; Seki et al., 2010), changes in orbital forcing of climate (Maslin et al., 1998) and tectonics (Raymo and Ruddiman, 1992; Cane and Molnar, 2001), increased stratification in the sub-arctic North Pacific (Haug et al., 2005), and reduced zonal sea-surface temperature gradients in the equatorial Pacific Ocean (Fedorov et al., 2006).

Regardless of the ultimate trigger, this study provides another solid contribution to the general agreement that all major Northern Hemisphere ice sheets responded simultaneously to the irreversible "climate crash" at 2.74 Ma sensu Bartoli et al. (2005) and extended beyond the coastline, most likely towards the shelf edge. However, what is overseen in this context of increased thermohaline circulation, moisture supply, and other feedbacks mechanisms for building up a large-scale continental ice sheet in the Northern Hemisphere, is whether an orogenic influence on regional climate was created on landmasses adjacent to the warm Pliocene North Atlantic Ocean (Foster et al., 2010). To become a potential host of continental ice, extensive plateau surfaces must pass a criti-

cal threshold altitude allowing a positive mass balance for glacial growth. Climate simulations have shown that with half the modern global topography, threshold pCO$_2$ values necessary for sustained glaciation in the Northern Hemisphere are lowered from 280 ppmv to 140–210 ppmv (DeConto et al., 2008). In the following, new empirical data from the Yermak Plateau are discussed in the light of late Miocene/early Pliocene uplift of the western European margin (Green and Duddy, 2010) that ultimately played an important role in priming the climate for the INHG during the late Pliocene.

5.2. Glacial growth at ~4 Ma in response to non-glacial tectonic uplift in the gateway region

In the Atlantic–Arctic gateway region, the INHG is expressed both by prominent IRD events (this study) and development of large prograding wedges along the margins at ~2.7 Ma (Dahlgren et al., 2005). Prior to the INHG, climate deterioration associated with long-term global cooling and epeirogenic uplift is subsequently deduced from erosional-driven changes in terrigenous sediment supply and its sources as well as changes in vegetation cover of the exposed landmasses. Distinct input of fine sands (63–100 μm) associated with enhanced Zr/K ratios occur between 5.8 and 4.1 Ma on the crest of the Yermak Plateau (Hole 910C) (Fig. 7). The most likely source for these sediments is the Devonian Old Redstone on northern Svalbard as indicated by distinct Zr/K anomalies in floodplain sediments within this geological province (Supplementary Fig. S5) (Ottesen et al., 2010). The fine sands are associated with highest concentration of pollen assemblages (Willard, 1996; Schafstall, 2011) and fresh organic plant materials as indicated by enhanced C/N ratios (>12) and low $\delta^{13}C_{org}$ values (−25‰) (Fig. 7). The regular occurrence of the fresh water algae *Botryococcus* in these sediments (Grøsfjeld et al., 2013) indicate deposition in a near-shore marine environment, strongly influenced by river plumes and associated terrestrial sediment transport. Pliocene terrestrial palynoflora indicate the presence of boreal forest to subarctic tundra in the source area (Willard, 1996; Schafstall, 2011). The inferred proximity to the shoreline, and (glacial-) fluvial sediment transport to the shelf break suggest the sub-aerially exposed, vegetated Barents Sea region as the most likely source of the terrestrial organic-rich fine sands during the latest Miocene–early Pliocene (Fig. 8). It supports inferences by Dahlgren et al. (2005) that (glacial-) fluvial erosion of weathering mantles of Mesozoic and early Cenozoic age resulted in the deposition of sandy-rich material along the continental margin prior to onset of large-scale glacial erosion in the Svalbard/Barents Sea area (Forsberg et al., 1999; Butt et al., 2000).

An abrupt drop in fine sands occurs at ~4 Ma and marks the upper boundary of gradually decreasing C/N and Zr/K ratios (Fig. 7). From ~4 Ma onwards, C/N ratios <10 and $\delta^{13}C_{org}$ values <−24.5‰ indicate input of more reworked (old) terrigenous organic matter. Parallel low Zr/K ratios associated with more fine-grained sediments are consistent with changes in amount and source of terrigenous sediments as a result of environmental changes in the hinterland (Fig. 7). Indeed, short-term pulses of Ti-rich sediments (high Ti/K ratios) are observed during minor cooling phases prior to 4.0 Ma (e.g. MIS Si4) (Fig. 7), however, short-term pulses occur more frequently between ~4.0 and 2.5 Ma. These Ti-rich sediments either originated from the Scandinavian mainland or – more likely – from Proterozoic deposits on western/northern Svalbard (Supplementary Fig. S6) (Ottesen et al., 2000, 2010; Salminen et al., 2004). High frequencies of Ti-rich sediment pulses together with enhanced input of reworked organic matter mark a gradual transition from densely vegetated to more glaciated landmasses on the exposed hinterland during the early Pliocene. It reflects the progressive glacial erosion of non-weathered bedrock, contrasting the (glacial-) fluvial erosion of (Zr-rich) weathering
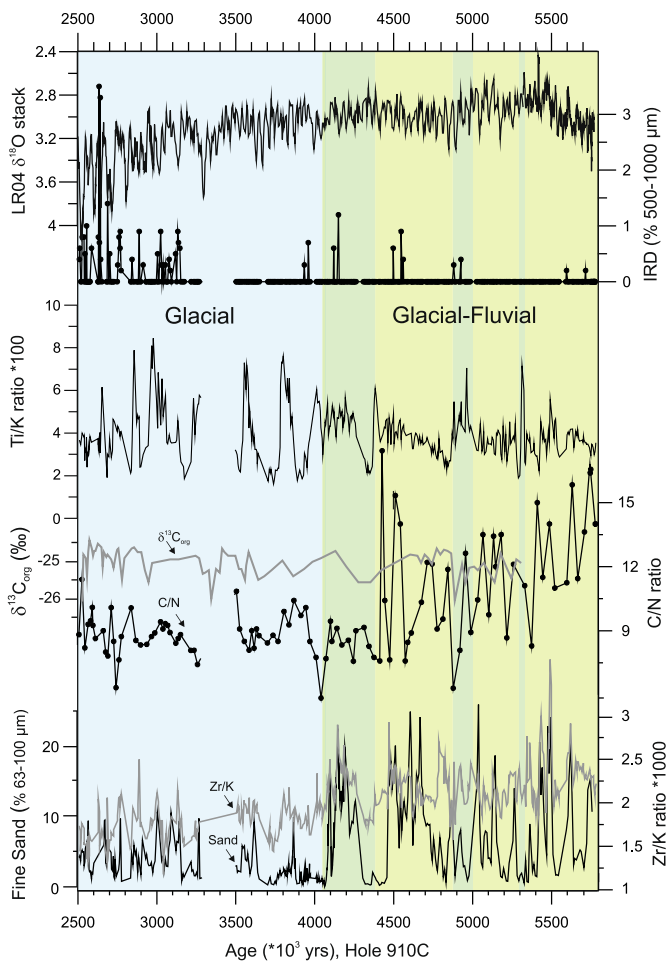
Fig. 7. Terrigenous sediment supply in the Atlantic–Arctic gateway region inferred from proxy data of Hole 910C between 5.8 and 2.5 Ma. From top to bottom: LR04 isotope stack (Lisiecki and Raymo, 2005), IRD (wt.% 500–1000 µm), Ti/K ratio, Carbon/Nitrogen (C/N) ratio supported by published $\delta^{13}C_{org}$ record of Hole 911A (Knies et al., 2002), and fine sand content (wt.% 63–100 µm) supported by the Zr/K ratio. Green color bars: Periods dominated by glacial–fluvial processes (prior to ~4 Ma). Blue color bars: Periods dominated by glacial processes (after ~4 Ma). (For interpretation of the references to color in this figure legend, the reader is referred to the web version of this article.)

coatings and vegetated landmasses prior to 4 Ma. Excluding the possibility of an unconformity (hiatus) based on seismic interpretation (Mattingsdal et al., 2013) and lithological description (Myhre et al., 1995), we propose that the abrupt drop in fine sands, associated decline in terrestrial organic matter supply and distinct change in sediment provenance at ~4 Ma are the result of less available material to be eroded from the hinterland due to progressive climate deterioration and initial glacial ice build-up.

Whether the abrupt change in the sediment composition also reflects re-routing of sediments induced by uplift and tilting, remains currently a matter of debate. The rapid post-5 Ma cooling phase on Svalbard is generally attributed to erosional response of glaciations (Dore and Jensen, 1996; Blythe and Kleinspehn, 1998; Anell et al., 2009). However, since large-scale glaciations did not evolve before 2.74 Ma on Svalbard (this study), and ~1.5 Ma in the Barents Sea (Laberg et al., 2010), a tectonic component of uplift during the early Pliocene cannot be ruled out completely (Anell et al., 2009; Green and Duddy, 2010). Vågnes et al. (1992) concluded that after removal of the glacial effect, tectonic uplift in the NW Barents Sea appears to be in the order of ~1000 m. Interestingly, Geissler and Jokat (2004) do not find indications for large-scale development of slope aprons associated with glacial trough mouth

fans after the INHG along the northern Svalbard margin. It may indicate that glacial ice covering the area transported/eroded less material from the hinterland and that sediment transfer mainly occurred through ice streams towards the south (e.g. Storfjord/Bear Island trough) and east/northeast (e.g. Frans Victoria trough).

5.3. The formation of an early Pliocene deep-water passage in the Atlantic–Arctic gateway

A critical component in this scenario of non-glacial uplift (and subsidence) is the final opening (deepening) of the Atlantic–Arctic gateway, i.e. the Fram Strait. Jokat et al. (2008) and later Hegewald and Jokat (2013) suggested the existence of a shallow water connection in the Fram Strait already during the late Oligocene. Jakobsson et al. (2007) proposed a widening of the Fram Strait since ~17.5 Ma to a passage deeper than 2000 m at ~13.7 Ma. Alternatively, Poirier and Hillaire-Marcel (2011) suggested an initial water mass exchange through a "proto-Fram Strait" already 36 Ma ago. Regardless of the initial opening, a true deep-water passage may not have existed before 7.5 to 5.0 Ma (Lawver et al., 1990; Kristoffersen, 1990). Further south, ongoing subsidence of the Greenland–Scotland Ridge through late Miocene time allowed increased export of North Atlantic Deep Water (NADW) to the Atlantic Ocean (Poore et al., 2006).

While parts of the Greenland–Scotland Ridge (i.e. Denmark Strait, Iceland–Faroe Ridge) were probably sub-aerially exposed prior to middle Miocene times (Poore et al., 2006), it is important to note that the Hovgård Ridge in the central Fram Strait restricted the unlimited through-flow of surface and deep-water masses until the late Miocene (Fig. 8). This ridge was sub-aerially exposed at least from ~25 Ma to ~6.7 Ma as inferred from a distinct unconformity in ODP Site 908 (Myhre et al., 1995; Matthiessen et al., 2009b). Enrichments of coarse sands (500–1000 µm) deposited above the unconformity between ~6.7 and 4.7 Ma in Hole 908A (Fig. 9) indicate proximal transport of eroded sediments during gradual subsidence of the Hovgård Ridge. The latter is supported by high concentrations of terrestrial plant tissue fragments in the same interval, indicating proximity to vegetated continental source (Poulsen et al., 1996). The sands are likely of non-glacial origin as indicated by constantly low Zr/K ratios (Fig. 9). The fine fraction in this sequence is dominated by smectite (Fig. 9) suggested to be derived from various point sources in the Arctic (e.g. Siberian Putorana flood basalts) and North Atlantic (Iceland–Faeroe Ridge), coupled to minor input of primary clay minerals (illite/chlorite) due to less severe weathering conditions during the late Miocene (Winkler et al., 2002). However, we propose that concomitant to the enrichments of non-glacial sands (500–1000 µm), that are mainly composed of igneous and volcanic rock fragments (Wolf-Welling et al., 1996), the smectite-rich fines are mainly of local origin. Findings of thick ash-layer derived glauconite beds above the hiatus in Hole 908A (Myhre et al., 1995) further support inferences of a nearby volcanic source for the smectite enrichments. Potential sources may be the Miocene plateau basalts, NW Spitsbergen (Prestvik, 1978), the Eocene Vestbakken Volcanic Province, W Barents Sea (Faleide et al., 1988), or the Hovgård Ridge itself. Indeed, Eldholm and Myhre (1977) and later Engen et al. (2008) and Ehlers and Jokat (2009) concluded from free-air gravity, magnetic, and seismic data that parts of the Hovgård Ridge are likely of volcanic origin, although the transition from ultraslow oceanic to continental crust is equivocal. Hermann and Jokat (2013) recently concluded that the Boreas Basin south of the Hovgård Ridge was formed in an ultraslow spreading regime. It supports the notion that the Hovgård Ridge may be a magmatic structure. According to this new magnetic and seismic data, the transpressional regime in the Fram Strait during the opening might have prevented a fast subsidence of the Hovgård Ridge.
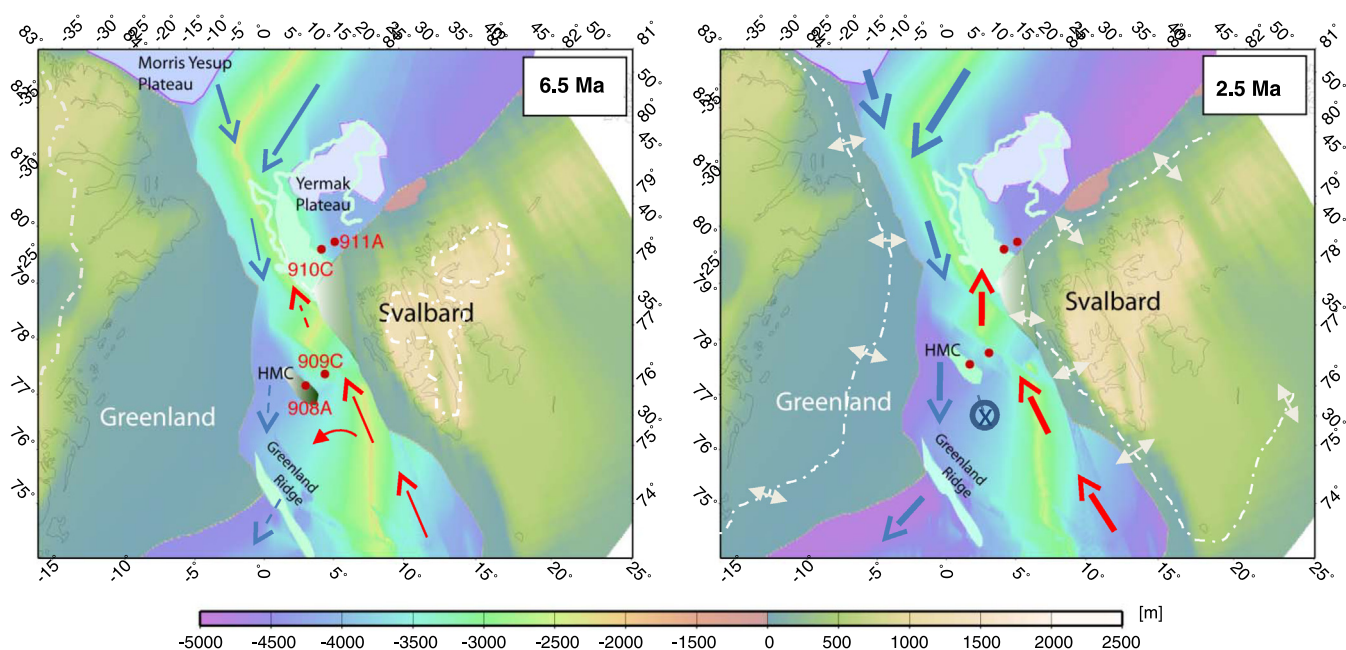
Fig. 8. Predicted paleobathymetry in the Fram Strait region for 6.5 Ma (left) and 2.5 Ma (right). The preglacial topography has been modified after Medvedev et al. (2013) and Knies and Gaina (2008). The Hovgård Ridge microcontinent (HMC) in the centre of the Fram Strait is sub-aerially exposed (6.5 Ma) and subsided to >2.5 km water depth (2.5 Ma). The Yermak Plateau is shown by the 2000 m present day bathymetric contour (light green line). The semi-transparent polygons show the extent of (stretched) continental crust and/or oceanic crust affected by Oligocene volcanism. Polygons outlined by magenta indicate the area of magnetic anomaly high intensity. The only ODP site situated on unequivocal oceanic crust, ODP Hole 909C, has a predicted depth of ca. 3000 m. Dashed white lines indicate the inferred glacial ice extent (modified after Solheim et al., 1998; Knies et al., 2009). Surface water exchange in the proto-Fram Strait is restricted during the late Miocene (6.5 Ma scenario) due to the blocking effect of the HMC. Widening/deepening of the Fram Strait during the Pliocene (2.5 Ma scenario) allow enhanced deep-water mass exchange and North Atlantic meridional overturning circulation. Blue arrows: cold Arctic water masses; red arrows: warm Atlantic water masses. Circled cross indicates location of modern deep-water formation.

Based on these observations we suggest that the slowly subsiding Hovgård Ridge – still a nearby source for the smectite-rich fines and volcanic rock fragments – limited the unrestricted deep-water exchange through the Atlantic–Arctic gateway until the early Pliocene. The timing confirms the minimum age (∼5 Ma) for the established deep-water (>2.5 km) circulation in the Fram Strait proposed by Lawver et al. (1990).

Contemporary to the inferred low saline Arctic through-flow associated with an enhanced northward flow of Pacific waters through the Bering Strait into the North Atlantic around 4.7 to 4.5 Ma (Haug et al., 2001; Verhoeven et al., 2011), a distinct increase in the supply of glacially derived sediments expressed by higher Zr/K and gradually decreasing smectite/illite ratios occurred in the Fram Strait at ∼4.7 Ma (Fig. 9). The deposition of these sediments mirrors the progressive climate cooling in the Arctic region and is likely the result of enhanced sea ice export associated with the establishment of the "modern-type" East Greenland Current, sometimes between ∼4.5 and 4.3 Ma (e.g. Bohrmann et al., 1990, updated to GTS 2012, Gradstein et al., 2012; Verhoeven et al., 2011). The observed changes in the proportions of coarse sands and abrupt appearance of gibbsite during the same time period (Fig. 9) are also indicative of changes in the circulation pattern in the Fram Strait. It suggests reduced proximity to the nearest source (Hovgård Ridge) and preferably deposition of sediments transported by ocean current from southerly sources (Fig. 8). The inferred uplift on the Barents Sea shelf during the early Pliocene and accompanied subsidence along the western passive margin (Ryseth et al., 2003) support a scenario whereby the Hovgård Ridge in the central Fram Strait subsided to depths that allowed unrestricted exchange of Atlantic and Arctic surface and deep-water masses (Fig. 8). The latter is supported by at least two observations. Firstly, based on Neodymium (Nd) isotope data, Haley et al. (2008) proposed that intermediate water exchange between the North Atlantic and the Arctic was limited throughout the period from ∼12 to ∼2 Ma. Considering the inadequacy of the

chronology and the low resolution of the late Neogene Nd record from the central Arctic Ocean (IODP Expedition 302) (Backman et al., 2008; Frank et al., 2008; Matthiessen et al., 2009b; O'Regan et al., 2010), however, an Arctic through-flow of North Atlantic intermediate waters prior to the proposed upper boundary (∼2 Ma) cannot be ruled out. Secondly, unrestricted deep-water mass exchange in the Fram Strait agrees with enhanced deep-water overflow from the Nordic Seas to the North Atlantic Ocean in the Early and Mid-Pliocene (Henrich et al., 2002; Poore et al., 2006). It supports inferences of enhanced production of North Atlantic Deep Water (NADW) after ∼4.7 Ma (Haug and Tiedemann, 1998; Ravelo and Andreasen, 2000).

5.4. Revised view on early Pliocene uplift and its role in INHG

The INHG culminated around 2.74 Ma after a long interval of climatic cooling (Zachos et al., 2001). The gradual reduction in the atmospheric pCO$_2$ is still regarded the primer for this global climatic deterioration (e.g. Lunt et al., 2008; Seki et al., 2010) although other feedback mechanisms maybe equally important (e.g. Raymo and Ruddiman, 1992; Maslin et al., 1998; Haug et al., 2005; Fedorov et al., 2006, 2013). The critical role of tectonic uplift in causing Cenozoic global cooling is widely acknowledged (Ruddiman, 1997), however its role in causing large-scale cooling in far-off polar regions remains unresolved (Ruddiman, 2010). Recently, Foster et al. (2010) showed from numerical simulations that small amounts of uplift of the North American Cordillera resulted in significant cooling of the North American continent during the late Miocene. It supports earlier inferences (e.g. Eyles, 1996) that mountain uplift in regions sensitive for the NHG was a vital precondition. In high northern latitudes, inconsistent timing of tectonic uplift events has hitherto hampered inferences on the effect of tectonically uplifted terrain on climate cooling (Eyles, 1996; Anell et al., 2009). However, exhumation beginning in the 7–5 Ma interval has been documented in a number of regions across the
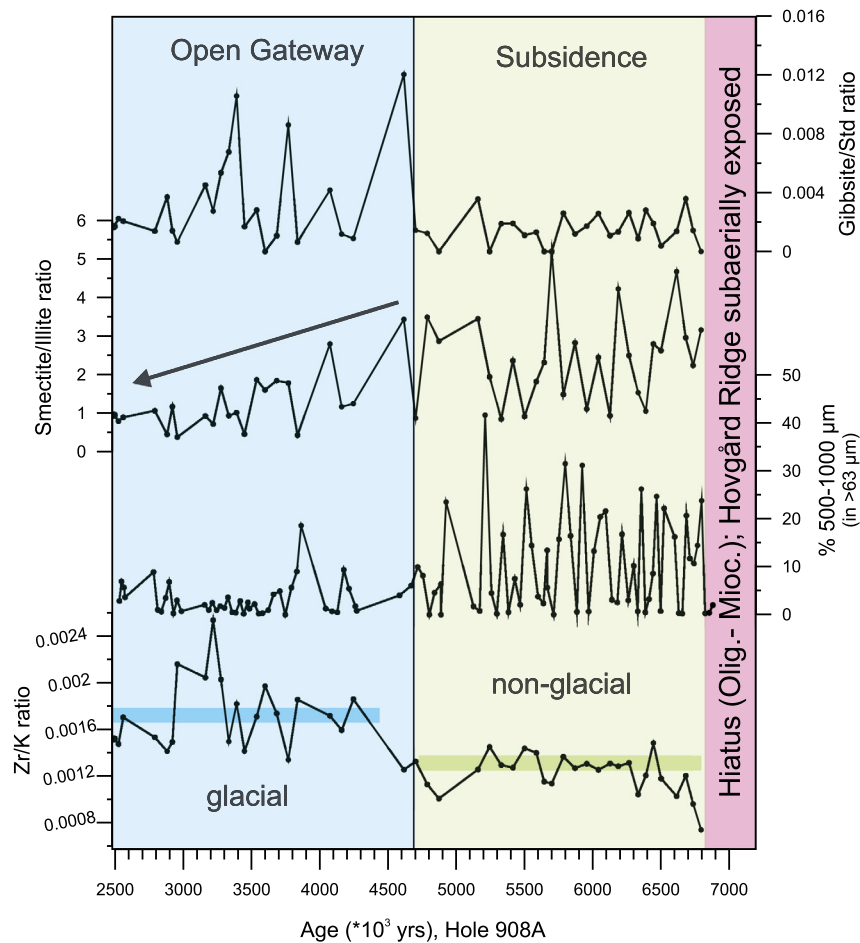
Fig. 9. Proxy data for terrigenous sediment supply in the central Fram Strait (ODP Hole 908A) between ~7.0 and 2.5 Ma. Pink bar indicates the upper boundary of the hiatus (~25 to ~6.7 Ma) in Hole 908A and inferred sub-aerial exposure of the Hovgård Ridge. Green bar indicates sediment characteristics during subsidence of the Hovgård Ridge. Low Zr/K ratios suggest a non-glacial environment. High amounts of coarse-grained material (% 500–1000 µm) enriched in volcanic fragments (Wolf-Welling et al., 1996) associated with smectite-rich fines indicate the erosional products from the Hovgård Ridge. Blue bar indicates a prominent shift towards a more glacially-influenced environment expressed by higher Zr/K and lower smectite/illite ratio. The abrupt appearance of gibbsite – expressed by the gibbsite/corundum (Gibbsite/Std) ratio in the <2 µm fraction – after ~4.7 Ma indicate a change in the circulation pattern in the central Fram Strait (see main text). (For interpretation of the references to color in this figure legend, the reader is referred to the web version of this article.)

Arctic and North Atlantic (Green and Duddy, 2010). Hence, the evidence of a timely consistent, non-glacial tectonic component, prior to the INHG, in a region that is sensitive to orbitally forced changes in solar irradiation, may reinforce the discussion of the role of high-latitude uplift events and associated cooling in far-off polar regions on the onset of major glaciations in the Northern Hemisphere.

Taking all observations from the Atlantic–Arctic regions together, we hypothesize a causal link between the abrupt changes in sediment properties at ~4 Ma and climate and tectonic feedback mechanisms prior to the INHG at ~2.7 Ma. We argue for a non-glacial, tectonic component in the Atlantic–Arctic gateway region during the latest Miocene–early Pliocene as documented by Green and Duddy (2010) that preconditioned the landscape adjacent to the northern North Atlantic/Nordic seas to host perennial ice fields and ultimately continental-scale ice. We support the hypothesis for tectonic uplift during the late Miocene/early Pliocene associated with the gradual build-up of continental ice at ~4 Ma in the NW Barents Sea by referring to regional tectonic uplift events along the entire NW European margin (Supplementary Fig. S7). Uplift of mainland Norway during the late Miocene/early Pliocene is reported by many studies (e.g. Green and Duddy, 2010). Formed by late Miocene uplift, subsequent tilting of shelf areas and submarine erosion in deep-water basins, the Intra-Neogene Unconformity (INU) of the Faroe–Shetland region is constrained to the

late early Pliocene (~4 ± 0.5 Ma) (Stoker et al., 2002, 2005). The uplift and (submarine) erosion in the Faroe–Shetland region may be correlated with the Molo Formation, a near-coastal sandy unit deposited in a wave dominated environment off Mid-Norway (Supplementary Fig. S7) (e.g. Henriksen et al., 2005). In part deposited during the late Miocene/early Pliocene (Eidvin et al., 2007), this unit is the result of compression and uplift of mainland Norway since the mid-Miocene (Henriksen et al., 2005). Further north, Sættem et al. (1994) and later Ryseth et al. (2003) argued that the non-depositional/erosional event (unconformity, ~2 Ma in duration) in the southwestern Barents Sea during the early Pliocene is due to regional uplift and concurrent sea level falls (Supplementary Fig. S7). More recently, Dörr et al. (2013) argued that the non-glacial uplift on Svalbard since the late Miocene is likely the result of thermal erosion of the mantle lithosphere under Svalbard (Vågnes and Amundsen, 1993).

This inferred tectonic uplift in the high northern latitudes during the late Miocene to early Pliocene corroborates the shoaling and restriction of deeper-water exchange via the CAS (Haug et al., 2001; Steph et al., 2006; Schmidt, 2007). The latter is associated with enhanced meridional overturning circulation coupled to increased poleward heat and moisture transport (e.g. Haug and Tiedemann, 1998). Enhanced NADW formation during the early Pliocene (Ravelo and Andreasen, 2000; Poore et al., 2006) is consistent with the observation of a "true" deep-water passage in the
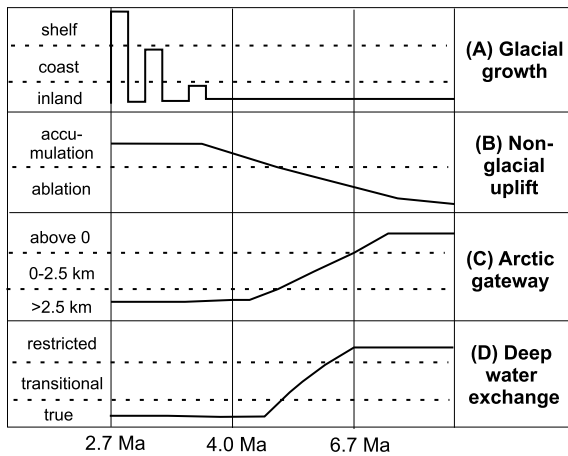
Fig. 10. Schematic summary of paleoclimatic and tectonic events during the Pliocene in the Arctic–Atlantic gateway region. (A) Build-up of the northern Svalbard/Barents Sea ice sheet. (B) Non-glacial uplift in NW-Europe during the late Miocene/early Pliocene. Stippled line indicates the inferred threshold for snow accumulation and ultimately glacial growth. (C) Subsidence of the Hovgård Ridge and widening/deepening of the central Fram Strait. (D) Inferred deep-water mass exchange through the Arctic–Atlantic gateway.

Atlantic–Arctic gateway since ∼5 Ma (Fig. 10). The efficiency of the "conveyer belt" heat pump may be counterbalanced by increased flow of low saline Arctic water from the Bering Strait to the Atlantic–Arctic gateway region since ∼4.7–4.5 Ma (Haug et al., 2001; Sarnthein et al., 2009; Verhoeven et al., 2011). With the cooling of elevated plateaus as a consequence of early Pliocene tectonic uplift of NW European mountain ranges next to the warm Pliocene North Atlantic Ocean ($\geqslant 3\,°C$ compared to modern SST) (Dowsett et al., 2012), additional moisture supply may have stimulated accumulation of extensive snow fields and ultimately the growth of large-scale ice sheets in the Northern Hemisphere 2.7 million years ago (Fig. 10).

6. Conclusions

Based on a well-constrained Pliocene chronology from the Atlantic–Arctic gateway, we support a consistent non-glacial, tectonic uplift component along the entire NW European margin during the late Miocene/early Pliocene (Green and Duddy, 2010). An abrupt change in sediment supply and source at ∼4 Ma is interpreted to present a critical climatic threshold when elevated plateaus became available to host perennial ice fields and ultimately continental scale ice (Fig. 10). Our data further suggest that the final deepening/widening of the Arctic–Atlantic gateway, the Fram Strait, between 6.5 and 5 Ma gradually caused more deepwater mass exchange that, in turn, likely contributed to the intensification of the North Atlantic thermohaline circulation (Fig. 10). The finding of high-standing plateaus adjacent to a warm Pliocene North Atlantic (Dowsett et al., 2012) in areas that are most sensitive to orbitally forced changes in solar irradiation provide a new dimension to the debate on whether early Pliocene tectonic uplift in high northern latitudes is indeed one decisive component for the onset of major Northern Hemisphere ice sheet expansion about 2.74 Ma ago (Ruddiman, 2010).

Appendix A. Supplementary material

Supplementary material related to this article can be found online at http://dx.doi.org/10.1016/j.epsl.2013.11.007.

References

Anell, I., Thybo, H., Artemieva, I.M., 2009. Cenozoic uplift and subsidence in the North Atlantic region: Geological evidence revisited. Tectonophysics 474, 78–105.

Backman, J., Moran, K., 2009. Expanding the Cenozoic paleoceanographic record in the Central Arctic Ocean: IODP Expedition 302 Synthesis. Centr. Eur. J. Geosci. 1 (2), 157–175. http://dx.doi.org/10.2478/v10085-009-0015-6.

Backman, J., Jakobsson, M., Frank, M., Sangiorgi, F., Brinkhuis, H., Stickley, C., O'Regan, M., Lovlie, R., Palike, H., Spofforth, D., Gattacecca, J., Moran, K., King, J., Heil, C., 2008. Age model and core-seismic integration for the Cenozoic Arctic Coring Expedition sediments from the Lomonosov Ridge. Paleoceanography 23. http://dx.doi.org/10.1029/2007pa001476. Pa1s03.

Ballantyne, A.P., Greenwood, D.R., Damste, J.S.S., Csank, A.Z., Eberle, J.J., Rybczynski, N., 2010. Significantly warmer Arctic surface temperatures during the Pliocene indicated by multiple independent proxies. Geology 38, 603–606.

Bartoli, G., Sarnthein, M., Weinelt, M., Erlenkeuser, H., Garbe-Schonberg, D., Lea, D.W., 2005. Final closure of Panama and the onset of northern hemisphere glaciation. Earth Planet. Sci. Lett. 237, 33–44.

Bartoli, G., Hönisch, B., Zeebe, R.E., 2011. Atmospheric CO_2 decline during the Pliocene intensification of Northern Hemisphere glaciations. Paleoceanography 26. http://dx.doi.org/10.1029/2010PA002055. PA4213.

Blythe, A.E., Kleinspehn, K.L., 1998. Tectonically versus climatically driven Cenozoic exhumation of the Eurasian plate margin, Svalbard: Fission track analyses. Tectonics 17, 621–639.

Bohrmann, G., Henrich, R., Thiede, J., 1990. Miocene to Quaternary paleoceanography in the northern North Atlantic: Variability in carbonate and biogenic opal accumulation. In: Bleil, U., Thiede, J. (Eds.), Geological History of the Polar Ocean Arctic versus Antarctic. Kluver Academic Publishers, pp. 647–675.

Brown, B., Gaina, C., Müller, R.D., 2006. Circum-Antarctic palaeobathymetry: Illustrated examples from Cenozoic to recent times. Palaeogeogr. Palaeoclimatol. Palaeoecol. 231, 158–168.

Butt, F.A., Elverhøi, A., Solheim, A., Forsberg, C.F., 2000. Deciphering Late Cenozoic development of the western Svalbard Margin from ODP Site 986 results. Mar. Geol. 169, 373–390.

Cane, M.A., Molnar, P., 2001. Closing of the Indonesian seaway as a precursor to east African aridirication around 3–4 million years ago. Nature 411, 157–162.

Dahlgren, K.I.T., Vorren, T.O., Stoker, M.S., Nielsen, T., Nygård, A., Sejrup, H.P., 2005. Late Cenozoic prograding wedges on the NW European continental margin: their formation and relationship to tectonics and climate. Mar. Pet. Geol. 22, 1089–1110.

De Schepper, S., Head, M.J., 2013. New Late Cenozoic acritarchs: evolution, palaeoecology and correlation potential in high latitude oceans. J. Syst. Palaeontol.. http://dx.doi.org/10.1080/14772019.2013.783883.

De Schepper, S., Head, M.J., Groeneveld, J., 2009. North Atlantic Current variability through marine isotope stage M2 (circa 3.3 Ma) during the mid-Pliocene. Paleoceanography 24. http://dx.doi.org/10.1029/2008PA001725.

De Schepper, S., Groeneveld, J., Naafs, B.D.A., Van Renterghem, C., Hennissen, J., Head, M.J., Louwye, S., Fabian, K., 2013. Northern Hemisphere glaciation during the globally warm early Late Pliocene. PLoS ONE. http://dx.doi.org/10.1371/journal.pone.0081508.

DeConto, R.M., Pollard, D., Wilson, P.A., Palike, H., Lear, C.H., Pagani, M., 2008. Thresholds for Cenozoic bipolar glaciation. Nature 455, 652–656.

Dore, A.G., Jensen, L.N., 1996. The impact of late Cenozoic uplift and erosion on hydrocarbon exploration: Offshore Norway and some other uplifted basins. Glob. Planet. Change 12, 415–436.

Dörr, N., Clift, P.D., Lisker, F., Spiegel, C., 2013. Why is Svalbard an island? Evidence for two-stage uplift, magmatic underplating and mantle thermal anomalies. Tectonics 32, 1–14. http://dx.doi.org/10.1002/tect.20039.

Dowsett, H.J., Robinson, M.M., Haywood, A.M., Hill, D.J., Dolan, A.M., Stoll, D.K., Chan, W.L., Abe-Ouchi, A., Chandler, M.A., Rosenbloom, N.A., Otto-Bliesner, B.L., Bragg, F.J., Lunt, D.J., Foley, K.M., Riesselman, C.R., 2012. Assessing confidence in Pliocene sea surface temperatures to evaluate predictive models. Nat. Clim. Change 2, 365–371.

Driscoll, N.W., Haug, G.H., 1998. A short circuit in thermohaline circulation: A cause for northern hemisphere glaciation?. Science 282, 436–438.

Ehlers, B.M., Jokat, W., 2009. Subsidence and crustal roughness of ultra-slow spreading ridges in the northern North Atlantic and the Arctic Ocean. Geophys. J. Int. 177, 451–462.

Eidvin, T., Bugge, T., Smelror, M., 2007. The Molo Formation, deposited by coastal progradation on the inner Mid-Norwegian continental shelf, coeval with the Kai Formation to the west and the Utsira Formation in the North Sea. Nor. J. Geol. 87, 75–142.

Eldholm, O., Myhre, A.M., 1977. Hovgaard Fracture Zone. Årb.-Nor. Polarinst. 1976, 195–208.

Elverhøi, A., Andersen, E.S., Dokken, T., Hebbeln, D., Spielhagen, R., Svendsen, J.I., Sørflaten, M., Rørnes, A., Hald, M., Forsberg, C.F., 1995. The growth and decay of the late Weichselian ice sheet in western Svalbard and adjacent areas based on provenance studies of marine sediments. Quat. Res. 44, 303–316.

Engen, Ø., Faleide, J.I., Dyreng, T.K., 2008. Opening of the Fram Strait gateway: A review of plate tectonic constraints. Tectonophysics 450, 51–69.

Eyles, N., 1996. Passive margin uplift around the North Atlantic region and its role in Northern Hemisphere Late Cenozoic glaciation. Geology 24, 103–106.

Faleide, J.I., Myhre, A.M., Eldholm, O., 1988. Early Tertiary volcanism at the western Barents Sea margin. In: Morton, A.C., Parson, L.M. (Eds.), Early Tertiary Volcanism and the Opening of the NE Atlantic, pp. 135–146. Geol. Soc. Special Publication 39.

Fedorov, A.V., Dekens, P.S., McCarthy, M., Ravelo, A.C., deMenocal, P.B., Barreiro, M., Pacanowski, R.C., Philander, S.G., 2006. The Pliocene paradox (mechanisms for a permanent El Nino). Science 312, 1485–1489.

Fedorov, A.V., Brierley, C.M., Lawrence, K.T., Liu, Z., Dekens, P.S., Ravelo, C., 2013. Patterns and mechanisms of early Pliocene warmth. Nature 496, 43–49. http://dx.doi.org/10.1038/nature12003.

Forsberg, C.F., Solheim, A., Elverhoi, A., Jansen, E., Channell, J.E.T., Andersen, E.S., 1999. The depositional environment of the western Svalbard margin during the late Pliocene and the Pleistocene: Sedimentary facies changes at Site 986. In: Raymo, M., Jansen, E., Blum, P., Herbert, T.D. (Eds.), Proc. ODP, Sci. Results 162. Ocean Drilling Program, College Station, TX, pp. 233–246.

Foster, G.L., Lunt, D.J., Parrish, R.R., 2010. Mountain uplift and the glaciation of North America – a sensitivity study. Clim. Past 6, 707–717.

Frank, M., Backman, J., Jakobsson, M., Moran, K., O'Regan, M., King, J., Haley, B.A., Kubik, P.W., Garbe-Schonberg, D., 2008. Beryllium isotopes in central Arctic Ocean sediments over the past 12.3 million years: Stratigraphic and paleoclimatic implications. Paleoceanography 23. http://dx.doi.org/10.1029/2007pa001478. Pa1s02.

Fronval, T., Jansen, E., 1996. Late Neogene paleoclimates and paleoceanography in the Iceland–Norwegian Sea: Evidence from the Iceland and Vøring Plateaus. In: Thiede, J., Myhre, A.M., Firth, J.V., Johnson, G.L., Ruddiman, W.F. (Eds.), Proc. ODP, Sci. Results 151. Ocean Drilling Program, College Station, TX, pp. 455–468.

Geirsdóttir, Á., 2004. Extent and chronology of glaciations in Iceland; a brief overview of the glacial history. In: Ehlers, J., Gibbard, P.L. (Eds.), Quaternary Glaciations – Extent and Chronology, part I, Europe. In: Dev. Quat. Sci., vol. 2. Elsevier, Amsterdam, The Netherlands, pp. 175–182.

Geissler, W.H., Jokat, W., 2004. A geophysical study of the northern Svalbard continental margin. Geophys. J. Int. 158, 50–66.

Gradstein, F.M., Ogg, J.G., Schmitz, M., Ogg, G., 2012. The Geologic Time Scale 2012. Elsevier, Amsterdam.

Green, P.F., Duddy, R., 2010. Synchronous exhumation events around the Arctic including examples from Barents Sea and Alaska North Slope. In: Petroleum Geology Conference Series, vol. 7, 2010, pp. 633–644.

Grøsfjeld, K., de Schepper, S., Fabian, K., Husum, K., Baranwal, S., Andreassen, K., Knies, J., 2013. Dating and palaeoenvironmental reconstruction of Early Pliocene sediments from the Yermak Plateau ODP Hole 911A in the Arctic Ocean, NNW of Svalbard, based on marine palynology. Quat. Sci. Rev., in review.

Haley, B.A., Frank, M., Spielhagen, R.F., Eisenhauer, A., 2008. Influence of brine formation on Arctic Ocean circulation over the past 15 million years. Nat. Geosci. 1, 68–72.

Haug, G.H., Tiedemann, R., 1998. Effect of the formation of the Isthmus of Panama on Atlantic Ocean thermohaline circulation. Nature 393, 673–676.

Haug, G.H., Tiedemann, R., Zahn, R., Ravelo, A.C., 2001. Role of Panama uplift on oceanic freshwater balance. Geology 29, 207–210.

Haug, G.H., Ganopolski, A., Sigman, D.M., Rosell-Mele, A., Swann, G.E.A., Tiedemann, R., Jaccard, S.L., Bollmann, J., Maslin, M.A., Leng, M.J., Eglinton, G., 2005. North Pacific seasonality and the glaciation of North America 2.7 million years ago. Nature 433, 821–825.

Head, M.J., Norris, G., Mudie, P.J., 1989. Palynology and dinocyst stratigraphy of the Upper Miocene and lowermost Pliocene, ODP Leg 105, Site 646, Labrador Sea. In: Srivastava, S.P., Arthur, M., Clement, B., et al. (Eds.), Proc. ODP, Sci. Results 105. Ocean Drilling Program, College Station, TX, pp. 423–451.

Hebbeln, D., Henrich, R., Baumann, K.-H., 1998. Paleoceanography of the last interglacial/glacial cycle in the Polar North Atlantic. Quat. Sci. Rev. 17, 125–153.

Hegewald, A., Jokat, W., 2013. Relative sea level variations in the Chukchi region – Arctic Ocean – since the Late Eocene. Geophys. Res. Lett. 40, 1–5. http://dx.doi.org/10.1002/GRL.50182.

Henrich, R., Baumann, K.H., Huber, R., Meggers, H., 2002. Carbonate preservation records of the past 3 Myr in the Norwegian–Greenland Sea and the northern North Atlantic: implications for the history of NADW production. Mar. Geol. 184, 17–39.

Henriksen, S., Fichler, C., Grønlie, A., Henningsen, T., Laursen, I., Løseth, H., Ottesen, D., Prince, I., 2005. The Norwegian Sea during the Cenozoic. In: Wandas, B., et al. (Eds.), Onshore–Offshore Relationships on the North Atlantic Margin. Norwegian Petroleum Society, pp. 111–133. Special publication.

Henriksen, E., Bjørnseth, H., Hals, T.K., Heide, T., Kiryukhina, T., Kløvjan, O.S., Larssen, G.B., Ryseth, A.E., Rønning, K., Sollid, K., Stoupakova, A., 2011. Uplift and erosion of the greater Barents Sea: impact on prospectivity and petroleum systems. In: Spencer, A.M., Embry, A.F., Gautier, D.L., Stoupakova, A.V., Sørensen, K. (Eds.), Arctic Petroleum Geology. Geological Society, London, pp. 271–281.

Hermann, T., Jokat, W., 2013. Crustal structure of the Boreas Basin and the Knipovich Ridge at 76°N in the North Atlantic. Geophys. J. Int. 193 (3), 1399–1414. http://dx.doi.org/10.1093/gji/ggt048.

Hodell, D.A., Curtis, J.H., Sierro, F.J., Raymo, M.E., 2001. Correlation of late Miocene to early Pliocene sequences between the Mediterranean and North Atlantic. Paleoceanography 16, 164–178.

Holmes, M.A., 1998. Alteration of uppermost lavas and volcaniclastics recovered during Leg 152 to the east Greenland margin. In: Saunders, A.D., Larsen, H.C., Wise, S.W. (Eds.), Proc. ODP, Sci. Results 152. Ocean Drilling Program, College Station, TX, pp. 115–128.

Iaccarino, S.M., Bertini, A., Di Stefano, A., Ferraro, L., Gennari, R., Grossi, F., Lirer, F., Manzi, V., Menichetti, E., Lucchi, M.R., Taviani, M., Sturiale, G., Angeletti, L., 2008. The Trave section (Monte dei Corvi, Ancona, Central Italy): an integrated paleontological study of the Messinian deposits. Stratigraphy 5, 281–306.

Jakobsson, M., Backman, J., Rudels, B., Nycander, J., Frank, M., Mayer, L., Jokat, W., Sangiorgi, F., O'Regan, M., Brinkhuis, H., King, J., Moran, K., 2007. The early Miocene onset of a ventilated circulation regime in the Arctic Ocean. Nature 447, 986–990.

Jokat, W., Geissler, W., Voss, M., 2008. Basement structure of the north–western Yermak Plateau. Geophys. Res. Lett. 35. http://dx.doi.org/10.1029/2007GL032892. L05309.

Kameo, K., Sato, T., 2000. Biogeography of Neogene calcareous nannofossils in the Caribbean and the eastern equatorial Pacific – floral response to the emergence of the Isthmus of Panama. Marine Micropaleontology 39, 201–218.

Kleiber, H.P., Knies, J., Niessen, F., 2000. The Late Weichselian glaciation of the Franz Victoria Trough, northern Barents Sea: ice sheet extent and timing. Mar. Geol. 168, 25–44.

Kleiven, H.F., Jansen, E., Fronval, T., Smith, T.H., 2002. Intensification of Northern Hemisphere glaciation in the circum Atlantic region (3.5–2.4 Ma) – ice-rafted detritus evidence. Palaeogeogr. Palaeoclimatol. Palaeoecol. 184, 213–223.

Knies, J., Gaina, C., 2008. Middle Miocene ice sheet expansion in the Arctic – views from the Barents Sea. Geochem. Geophys. Geosyst. 9. http://dx.doi.org/10.1029/2007GC001824. Q02015.

Knies, J., Matthiessen, J., Vogt, C., Stein, R., 2002. Evidence of 'Mid-Pliocene (similar to 3 Ma) global warmth' in the eastern Arctic Ocean and implications for the Svalbard/Barents Sea ice sheet during the late Pliocene and early Pleistocene (similar to 3–1.7 Ma). Boreas 31, 82–93.

Knies, J., Matthiessen, J., Mackensen, A., Stein, R., Vogt, C., Frederichs, T., Nam, S.I., 2007. Effects of Arctic freshwater forcing on thermohaline circulation during the Pleistocene. Geology 35, 1075–1078.

Knies, J., Matthiessen, J., Vogt, C., Laberg, J.S., Hjelstuen, B.O., Smelror, M., Larsen, E., Andreassen, K., Eidvin, T., Vorren, T.O., 2009. The Plio-Pleistocene glaciation of the Barents Sea-Svalbard region: a new model based on revised chronostratigraphy. Quat. Sci. Rev. 28, 812–829.

Kristoffersen, Y., 1990. On the tectonic evolution and paleoceanographic significance of the Fram Strait Gateway. In: Bleil, U., Thiede, J. (Eds.), Geological History of the Polar Ocean Arctic versus Antarctic. Kluver Academic Publishers, pp. 63–76.

Laberg, J.S., Andreassen, K., Knies, J., Vorren, T.O., Winsborrow, M., 2010. Late Pliocene–Pleistocene development of the Barents Sea Ice Sheet. Geology 38, 107–110.

Laberg, J.S., Andreassen, K., Vorren, T.O., 2012. Late Cenozoic erosion of the high-latitude southwestern Barents Sea shelf revisited. Geol. Soc. Am. Bull. 124, 77–88.

Lawver, L.A., Müller, R.D., Srivastava, S.P., Roest, W., 1990. The opening of the Arctic Ocean. In: Bleil, U., Thiede, J. (Eds.), Geological History of the Polar Oceans: Arctic versus Antarctic. Kluwer Academic Press, Dordrecht/Boston/London, pp. 29–62.

Lisiecki, L.E., Raymo, M.E., 2005. A Pliocene–Pleistocene stack of 57 globally distributed benthic d18O records. Paleoceanography 20. PA1003.

Lunt, D.J., Foster, G.L., Haywood, A.M., Stone, E.J., 2008. Late Pliocene Greenland glaciation controlled by a decline in atmospheric CO(2) levels. Nature 454, 1102–1105.

Lunt, D.J., Haywood, A.M., Schmidt, G.A., Salzmann, U., Valdes, P.J., Dowsett, H.J., Loptson, C.A., 2012. On the causes of mid-Pliocene warmth and polar amplification. Earth Planet. Sci. Lett. 321–322, 128–138. http://dx.doi.org/10.1016/j.epsl.2011.12.042.

März, C., Schnetger, B., Brumsack, H.J., 2010. Paleoenvironmental implications of Cenozoic sediments from the central Arctic Ocean (IODP Expedition 302) using inorganic geochemistry. Paleoceanography 25. http://dx.doi.org/10.1029/2009pa001860. Pa3206.

Maslin, M.A., Li, X.S., Loutre, M.F., Berger, A., 1998. The contribution of orbital forcing to the progressive intensification of Northern Hemisphere glaciation. Quat. Sci. Rev. 17, 411–426.

Matthiessen, J., Knies, J., Vogt, C., Stein, R., 2009a. Pliocene palaeoceanography of the Arctic Ocean and subarctic seas. Philos. Trans. R. Soc. Lond. A 367, 21–48.

Matthiessen, J., Brinkhuis, H., Poulsen, N., Smelror, M., 2009b. Decahedrella martinheadii Manum 1997 – a stratigraphically and paleoenvironmental useful Miocene acritarch of the high northern latitudes. Micropaleontology 55, 171–186.

Mattingsdal, R., Knies, J., Andreassen, K., Fabian, K., Husum, K., Grøsfjeld, K., de Schepper, S., 2013. A new 6 Myr stratigraphic framework for the Atlantic–Arctic gateway. Quat. Sci. Rev.. http://dx.doi.org/10.1016/j.quascirev.2013.08.022.

McKay, R., Naish, T., Carter, L., Riesselman, C., Dunbar, R., Sjunneskog, C., Winter, D., Sangiorgi, F., Warren, C., Pagani, M., Schouten, S., Willmott, V., Levy, R., DeConto, R., Powell, R.D., 2012. Antarctic and Southern Ocean influences on Late Pliocene global cooling. Proc. Natl. Acad. Sci. USA 109, 6423–6428.

Medvedev, S., Souche, A., Hartz, E., 2013. Influence of ice sheet and glacial erosion on passive margins of Greenland. Geomorphology 193, 36–46. http://dx.doi.org/10.1016/j.geomorph.2013.03.029.

Moran, K., Backman, J., Brinkhuis, H., Clemens, S.C., Cronin, T., Dickens, G.R., Eynaud, F., Gattacceca, J., Jakobsson, M., Jordan, R.W., Kaminski, M., King, J., Koc, N., Krylov, A., Martinez, N., Matthiessen, J., McInroy, D., Moore, T.C., Onodera, J., O'Regan, M., Palike, H., Rea, B., Rio, D., Sakamoto, T., Smith, D.C., Stein, R., St John, K., Suto, I., Suzuki, N., Takahashi, K., Watanabe, M., Yamamoto, M., Farrell, J., Frank, M., Kubik, P., Jokat, W., Kristoffersen, Y., 2006. The Cenozoic palaeoenvironment of the Arctic Ocean. Nature 441, 601–605.

Mudelsee, M., Raymo, M.E., 2005. Slow dynamics of the Northern Hemisphere glaciation. Paleoceanography 20. http://dx.doi.org/10.1029/2005pa001153. Pa4022.

Müller, R.D., Sdrolias, M., Gaina, C., Steinberger, B., Heine, C., 2008. Long-term sea-level fluctuations driven by ocean basin dynamics. Science 319, 1357–1362.

Myhre, A.M., Thiede, J., Firth, J.V., et al., 1995. Proceedings ODP, Initial Reports 151. Ocean Drilling Program, College Station, TX.

Naish, T., Powell, R., Levy, R., Wilson, G., Scherer, R., Talarico, F., Krissek, L., Niessen, F., Pompilio, M., Wilson, T., Carter, L., DeConto, R., Huybers, P., McKay, R., Pollard, D., Ross, J., Winter, D., Barrett, P., Browne, G., Cody, R., Cowan, E., Crampton, J., Dunbar, G., Dunbar, N., Florindo, F., Gebhardt, C., Graham, I., Hannah, M., Hansaraj, D., Harwood, D., Helling, D., Henrys, S., Hinnov, L., Kuhn, G., Kyle, P., Laufer, A., Maffioli, P., Magens, D., Mandernack, K., McIntosh, W., Millan, C., Morin, R., Ohneiser, C., Paulsen, T., Persico, D., Raine, I., Reed, J., Riesselman, C., Sagnotti, L., Schmitt, D., Sjunneskog, C., Strong, P., Taviani, M., Vogel, S., Wilch, T., Williams, T., 2009. Obliquity-paced Pliocene West Antarctic ice sheet oscillations. Nature 458, 322–328.

Nizou, J., Hanebuth, T.J.J., Vogt, C., 2011. Deciphering signals of late Holocene fluvial and aeolian supply from a shelf sediment depocentre off Senegal (north–west Africa). J. Quat. Sci. 26 (4), 411–421. http://dx.doi.org/10.1002/jqs.1467.

O'Regan, M., St John, K., Moran, K., Backman, J., King, J., Haley, B.A., Jakobsson, M., Frank, M., Rohl, U., 2010. Plio-Pleistocene trends in ice rafted debris on the Lomonosov Ridge. Quat. Int. 219, 168–176.

Ottesen, R.T., Bogen, J., Bølviken, B., Volden, T., Haugland, T., 2000. Geochemical Atlas of Norway. Part 1: Geochemical Atlas of Norway – Geochemical Composition of Overbank Sediments. Geological Survey of Norway (NGU), Trondheim, Norway.

Ottesen, R.T., Bogen, J., Finne, T.E., Andersson, M., Dallmann, W.K., Eggen, O.A., Jartun, M., Lundkvist, Q., Pedersen, H.R., Volden, T., 2010. Geochemical Atlas of Norway. Part 2: Geochemical Atlas of Spitsbergen – Geochemical Composition of Overbank Sediments. Geological Survey of Norway (NGU), Trondheim, Norway.

Poirier, A., Hillaire-Marcel, C., 2011. Improved Os-isotope stratigraphy of the Arctic Ocean. Geophys. Res. Lett. 38. http://dx.doi.org/10.1029/2011gl047953. L14607.

Poore, H.R., Samworth, R., White, N.J., Jones, S.M., McCave, I.N., 2006. Neogene overflow of Northern Component Water at the Greenland–Scotland Ridge. Geochem. Geophys. Geosyst. 7. http://dx.doi.org/10.1029/2005gc001085. Q06010.

Poulsen, N.E., Manum, S.B., Williams, G.L., Ellegaard, M., 1996. Tertiary dinoflagellate biostratigraphy of Sites 907, 908, and 909 in the Norwegian–Greenland Sea. In: Thiede, J., Myhre, A.M., Firth, J.V., Johnson, G.L., Ruddiman, W.F. (Eds.), Proc. ODP, Sci. Results 151. Ocean Drilling Program, College Station, TX, pp. 255–288.

Powell, A.J., Brinkhuis, H., 2004. Figure 21.2. In: Lourens, L., Hilgen, F., Shackleton, N.J., Laskar, J., Wilson, D., 2004. The neogene period. In: Gradstein, F., Ogg, J., Smith, A. (Eds.), A Geological Time Scale 2004. Cambridge University Press, Cambridge, UK, pp. 409–440.

Prestvik, T., 1978. Cenozoic plateau lavas of Spitsbergen – a geochemical study. Årb.-Nor. Polarinst. 1977, 129–143.

Ravelo, A.C., Andreasen, D.H., 2000. Enhanced circulation during a warm period. Geophys. Res. Lett. 27, 1001–1004.

Raymo, M.E., Ruddiman, W.F., 1992. Tectonic forcing of late Cenozoic climate. Nature 359, 117–122.

Robinson, M.M., Valdes, P.J., Haywood, A.M., Dowsett, H.J., Hill, D.J., Jones, S.M., 2011. Bathymetric controls on Pliocene North Atlantic and Arctic sea surface temperature and deepwater production. Palaeogeogr. Palaeoclimatol. Palaeoecol. 309, 92–97.

Ruddiman, W.F. (Ed.), 1997. Tectonic Uplift and Climate Change. Plenum Press, New York, USA. 537 pp.

Ruddiman, W.F., 2010. A Paleoclimatic Enigma?. Science 328, 838–839.

Ruddiman, W.F., Kutzbach, J.E., 1989. Forcing of late Cenozoic northern Hemisphere climate by plateau uplift in southern Asia and the American West. J. Geophys. Res., Atmos. 94, 18409–18427.

Ryseth, A., Augustson, J.H., Charnock, M., Haugerud, O., Knutsen, S.-M., Midbøe, P.S., Opsal, J.G., Sundsbø, G., 2003. Cenozoic stratigraphy and evolution of the Sørvestsnaget Basin, southwestern Barents Sea. Nor. J. Geol. 83, 107–130.

Salminen, R., Chekushin, V., Tenhola, M., Bogatyrev, I., Glavatskikh, S.P., Fedotova, E., Gregorauskiene, V., Kashulina, G., Niskavaara, H., Polischuok, A., Rissanen, K., Slenok, L., Tomilina, O., Zhdanova, L., 2004. Geochemical Atlas of the Eastern Barents Region. Elsevier. 548 pp.

Sarnthein, M., Bartoli, G., Prange, M., Schmittner, A., Schneider, B., Weinelt, M., Andersen, N., Garbe-Schönberg, D., 2009. Mid-Pliocene shifts in ocean overturning circulation and the onset of Quaternary-style climates. Clim. Past 5, 269–283.

Sato, T., Kameo, K., 1996. Pliocene to Quaternary calcareous nannofossil biostratigraphy of the Arctic Ocean, with reference to late Pliocene glaciation. In: Thiede, J., Myhre, A.M., Firth, J.V., Johnson, G.L., Ruddiman, W.F. (Eds.), Proc. ODP, Sci. Results 151. Ocean Drilling Program, College Station, TX, pp. 39–59.

Sato, T., Yuguchi, S., Takayama, T., Kameo, K., 2004. Drastic change in the geographical distribution of the cold-water nannofossil Coccolithus pelagicus (Wallich) Schiller at 2.74 Ma in the late Pliocene, with special reference to glaciation in the Arctic Ocean. Marine Micropaleontology 52, 181–193.

Sættem, J., Bugge, T., Fanavoll, S., Goll, R.M., Mork, A., Mork, M.B.E., Smelror, M., Verdenius, J.G., 1994. Cenozoic margin development and erosion of the Barents Sea – core evidence from southwest of Bjørnøya. Mar. Geol. 118, 257–281.

Schafstall, N., 2011. The pollen records from ODP Hole 910C and 911A near Svalbard. Master Thesis. Department of Biology, Utrecht University, The Netherlands. 43 pp.

Schmidt, D., 2007. The closure history of the Central American seaway: evidence from isotopes and fossils to models and molecules. In: Williams, M., Haywood, A.D., Gregory, F., Schmidt, D. (Eds.), Deep-Time Perspectives on Climate Change: Marrying the Signal from Computer Models and Biological Proxies. Geological Society of London, pp. 427–442. TMS special publication.

Schreck, M., Matthiessen, J., Head, M.J., 2012. A magnetostratigraphic calibration of Middle Miocene through Pliocene dinoflagellate cyst and acritarch events in the Iceland Sea (Ocean Drilling Program Hole 907A). Rev. Palaeobot. Palynol. 187, 66–94.

Seki, O., Foster, G.L., Schmidt, D.N., Mackensen, A., Kawamura, K., Pancost, R.D., 2010. Alkenone and boron-based Pliocene pCO(2) records. Earth Planet. Sci. Lett. 292, 201–211.

Shackleton, N.J., Backman, J., Zimmerman, H., Kent, D.V., Hall, M.A., Roberts, D.G., Schnitker, D., Baldauf, J.G., Desprairies, A., Homrighausen, R., Huddlestun, P., Keene, J.B., Kaltenback, A.J., Krumsieck, K.A.O., Morton, A.C., 1984. Oxygen isotope calibration of the onset of ice-rafting and history of glaciation in the North Atlantic region. Nature 307, 620–623.

Solheim, A., Faleide, J.I., Andersen, E.S., Elverhøi, A., Forsberg, C.F., Vanneste, K., Uenzelmann-Neben, G., Channell, J.E.T., 1998. Late Cenozoic seismic stratigraphy and glacial geological development of the East Greenland and Svalbard–Barents Sea continental margin. Quat. Sci. Rev. 17, 155–184.

Spiegler, D., 1996. Planktonic foraminifer Cenozoic biostratigraphy of the Arctic Ocean, Fram Strait (Sites 908–909), Yermak Plateau (Sites 910–912), and east Greenland margin (Site 913). In: Thiede, J., Myhre, A.M., Firth, J.V., Johnson, G.L., Ruddiman, W.F. (Eds.), Proc. ODP, Sci. Results 151. Ocean Drilling Program, College Station, TX, pp. 153–167.

Stein, R., 2008. Arctic Ocean Sediments: Processes, Proxies, and Paleoenvironment. Dev. Mar. Geol., vol. 2. 608 pp.

Stein, R., Macdonald, R.W., 2004. The Organic Carbon Cycle in the Arctic Ocean. Springer-Verlag, Heidelberg, Berlin. 363 pp.

Steph, S., Tiedemann, R., Prange, M., Groeneveld, J., Nurnberg, D., Reuning, L., Schulz, M., Haug, G.H., 2006. Changes in Caribbean surface hydrography during the Pliocene shoaling of the Central American Seaway. Paleoceanography 21. http://dx.doi.org/10.1029/2004pa001092. Pa4221.

Stoker, M.S., Nielsen, T., van Weering, T.C.E., Kuijpers, A., 2002. Towards an understanding of the Neogene tectonostratigraphic framework of the NE Atlantic margin between Ireland and the Faroe Islands. Mar. Geol. 188, 233–248.

Stoker, M.S., Praeg, D., Hjelstuen, B.O., Laberg, J.S., Nielsen, T., Shannon, P.M., 2005. Neogene stratigraphy and the sedimentary and oceanographic development of the NW European Atlantic margin. Mar. Pet. Geol. 22, 977–1005.

Vågnes, E., Amundsen, H.E.F., 1993. Late Cenozoic Uplift and Volcanism on Spitsbergen: Caused by Mantle Convection?. Geology 21, 251–254. http://dx.doi.org/10.1130/0091-7613(1993)021.

Vågnes, E., Faleide, J.I., Gudlaugsson, S.T., 1992. Glacial erosion and tectonic uplift in the Barents Sea. Nor. Geol. Tidsskr. 72, 333–338.

Verhoeven, K., Louwye, S., 2012. Selenopemphix islandensis sp nov.: a new organic-walled dinoflagellate cyst from the Lower Pliocene Tjornes beds, northern Iceland. Palynology 36, 10–25.

Verhoeven, K., Louwye, S., Eiriksson, J., De Schepper, S., 2011. A new age model for the Pliocene–Pleistocene Tjörnes section on Iceland: Its implication for the timing of North Atlantic–Pacific paleoceanographic pathways. Palaeogeogr. Palaeoclimatol. Palaeoecol. 309, 33–52.

Wahsner, M., Mueller, C., Stein, R., Ivanov, G., Levitan, M., Shelekhova, E., Tarasov, G., 1999. Clay–mineral distribution in surface sediments of the Eurasian Arctic Ocean and continental margin as indicator for source areas and transport pathways – A synthesis. Boreas 28, 215–233.

Willard, D.A., 1996. Pliocene–Pleistocene pollen assemblages from the Yermak Plateau, Arctic Ocean: Sites 910 and 911. In: Thiede, J., Myhre, A.M., Firth, J.V., Johnson, G.L., Ruddiman, W.F. (Eds.), Proc. ODP, Sci. Results 151. Ocean Drilling Program, College Station, TX, pp. 297–305.

Winkelmann, D., Schäfer, C., Stein, R., Mackensen, A., 2008. Terrigenous events and climate history of the Sophia Basin, Arctic Ocean. Geochem. Geophys. Geosyst. 9 (7). http://dx.doi.org/10.1029/2008GC002038. Paper Q07023 (14 pp.).

Winkler, A., Wolf-Welling, T.C.W., Stattegger, K., Thiede, J., 2002. Clay mineral sedimentation in high northern latitude deep-sea basins since the Middle Miocene (ODP Leg 151, NAAG). Int. J. Earth Sci. 91, 133–148.

Wolf-Welling, T.C.W., Cremer, M., O'Connell, S., Winkler, A., Thiede, J., 1996. Cenozoic Arctic Gateway paleoclimate variability: indications from changes in coarse-fraction composition. In: Thiede, J., Myhre, A.M., Firth, J.V., Johnson, G.L., Ruddiman, W.F. (Eds.), Proc. ODP, Sci. Results 151. Ocean Drilling Program, College Station, TX, pp. 515–569.

Wollenburg, J.E., Kuhnt, W., Mackensen, A., 2001. Changes in Arctic Ocean paleoproductivity and hydrography during the last 145 kyr: The benthic foraminiferal record. Paleoceanography 16, 65–77.

Zachos, J., Pagani, M., Sloan, L., Thomas, E., Billups, K., 2001. Trends, rhythms, and aberrations in global climate 65 Ma to present. Science 292, 686–693.